Deep–Sea Research I 218 (2025) 104473

Contents lists available at ScienceDirect

Deep-Sea Research Part I

journal homepage: www.elsevier.com/locate/dsri

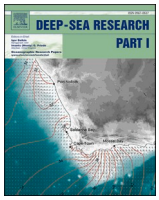

Trophic partitioning and mercury accumulation in deep-sea fishes of the East China Sea

Xinyu Chen [a], Zezheng Li [a], David Mboglen [a,d], Yunkai Li [a,b,c,*]

[a] College of Marine Living Resources and Management, Shanghai Ocean University, 999 Huchenghuan Rd., Shanghai, China
[b] The Key Laboratory of Sustainable Exploitation of Oceanic Fisheries Resources, Ministry of Education, 999 Huchenghuan Rd., Shanghai, China
[c] National Engineering Research Centre for Oceanic Fisheries, Shanghai Ocean University, 999 Huchenghuan Rd., Shanghai, China
[d] Institute of Agricultural Research for Development (IRAD), Specialized Research Station on Marine Ecosystems, Antenne d'Ebodjé, 219 Kribi, Cameroon

ARTICLE INFO

Keywords:
East China Sea
Deep-sea fish
Feeding ecology
Mercury
Trophic guilds

ABSTRACT

The deep sea, characterized by darkness, low temperatures, limited food availability, and extreme pressure, harbors a diverse array of life forms. Deep-sea fish, which have evolved unique adaptations to thrive in these harsh conditions, play a crucial role in marine ecosystems and biogeochemical cycles. This study investigated the trophic ecology and mercury (Hg) dynamics of eleven deep-sea fish species in the East China Sea (ECS) using stable isotope analysis (SIA) and total mercury (THg) concentration. Our findings revealed significant overlap in trophic niches among the examined species, with notable exceptions indicating instances of competition and resource partitioning. *Coelorhynchus anatirostris* exhibited a relatively broader trophic niche, suggesting a generalist feeding strategy, while *Chlorophthalmus albatrossis* and *Neoscopelus microchir* displayed more specialized niches. We identified four distinct trophic guilds based on $\delta^{13}C$ and $\delta^{15}N$ values, as well as THg concentrations, which underscore the complex interactions of niche differentiation and resource sharing within the deep-sea community. The incorporation of Hg as an additional bioindicator provided valuable insights into feeding strategies and trophic levels, highlighting its effectiveness in distinguishing ecological niches. Positive correlations between THg concentration and total length were observed in certain species, but not across all. At the community level, THg concentrations were closely associated with trophic level and habitat. Notably, THg concentrations in demersal fish were significantly lower than those in mesopelagic fish, likely attributable to the intricate distribution of THg within the ECS, suggesting the complexity of THg variation with depth. Our results demonstrate how vertical habitat partitioning and dietary preferences mediate competition and coexistence among deep-sea fish species in the ECS. These findings advance our understanding of deep-sea ecosystem trophic structure and function while providing insights for conservation and management strategies.

1. Introduction

The deep sea, recognized as Earth's largest habitat, encompasses billions of cubic kilometers. In contrast to shallow marine ecosystems, the deep-sea environment is characterized by low light levels, low temperatures, and limited food resources, which collectively shape its unique ecological attributes (Pethybridge et al., 2010; Drazen and Sutton, 2017). However, the biological diversity and biomass within deep-sea ecosystems are substantial (Cook et al., 2013).

Fish represent a crucial component of deep-sea ecosystems, primarily comprising mid-trophic level species (e.g., lanternfish, *Coelorinchus* spp.) that feed on zooplankton, small fish, and benthic organisms, as well as high-trophic level predators such as deep-sea sharks (Drazen and Sutton, 2017; Haddock and Choy, 2024). Based on depth distribution, deep-sea fish are classified into mesopelagic, demersal, bathypelagic, and abyssopelagic groups (Drazen and Sutton, 2017). Notably, mesopelagic fish account for approximately 95% of global fish biomass and perform diel vertical migration (DVM) between surface and deep-sea layers (Kaartvedt et al., 2012; Irigoien et al., 2014). During the night, they ascend to the surface waters to feed on zooplankton, crustaceans, and small fish, returning to deeper waters during the day, thereby facilitating the transfer of surface-derived nutrients and energy to deeper waters (Davison et al., 2013; Bernal et al., 2015; Prellezo et al., 2024). Demersal fish contribute to energy transfer by consuming

* Corresponding author. College of Marine Living Resources and Management, Shanghai Ocean University, 999 Huchenghuan Rd., Shanghai, China
E-mail address: ykli@shou.edu.cn (Y. Li).

https://doi.org/10.1016/j.dsr.2025.104473
Received 22 August 2024; Received in revised form 22 January 2025; Accepted 20 February 2025
Available online 21 February 2025

vertically migrating organisms, thereby facilitating the transport of nutrients, pollutants, and parasites from the upper zone to the seafloor—a process crucial for carbon sequestration and biogeochemical cycling in deep-sea ecosystems (Drazen and Sutton, 2017; Ñacari et al., 2023). While historically studied separately, the established migratory connectivity between mesopelagic and demersal fish communities necessitates an integrated research approach to comprehensively understand their collective role in maintaining deep-sea ecosystems functions (Drazen and Sutton, 2017).

Inland rivers deliver essential nutrients to the East China Sea (ECS), one of the largest marginal seas in the western Pacific Ocean, supporting a diverse array of fishery resources (Chen et al., 2016; Wang and Zhang, 2023). Numerous studies have documented a significant presence of deep-sea fish species, including *Diaphus* spp., *Myctophum* spp., and *Coelorinchus* spp., within the ECS (Okazaki and Nakata, 2007; Mei et al., 2019; Xu et al., 2019). Research has investigated various biological aspects of these species, such as biomass estimation (Davison et al., 2015), age and growth (Zhang and Guo, 2024), diet composition (Tanaka et al., 2013), and reproductive strategies (Sassa et al., 2016). However, the mechanisms by which deep-sea fishes partition resources to minimize competition remain understudied. Investigating niche partitioning is crucial for understanding the processes that facilitate the coexistence of deep-sea species. This knowledge is fundamental for advancing our understanding of population dynamics, resource use, and energy transfer within the deep-sea ecosystems. Additionally, it provides a foundation for developing fisheries management strategies that promote the sustainable exploitation of these valuable resources (Brandl et al., 2020).

Stable isotope analysis (SIA) and mercury (Hg) serve as valuable tools for understanding marine food web structure (Boecklen, 2011; Le Croizier et al., 2020). The ratio of $^{13}C/^{12}C$ ($\delta^{13}C$) commonly distinguishes and quantifies the relative contributions of various primary producers (e.g., pelagic vs. benthic) (Cherel and Hobson, 2007), while the ratio of $^{15}N/^{14}N$ ($\delta^{15}N$) is typically enriched in consumers relative to their diet, providing an estimate of trophic position (Caut et al., 2009). Released from both natural and anthropogenic sources, Hg represents a significant global pollutant that undergoes microbial conversion to methylmercury (MeHg) in marine environments (Obrist et al., 2018). MeHg's high affinity for adipose tissue and slow metabolic degradation leads to bioaccumulation and biomagnification through food webs (Gworek et al., 2016; Barbosa et al., 2022). Since dietary intake represents the primary pathway for Hg accumulation in marine organisms, Hg concentrations reflect feeding behaviors and serve as a complementary trophic tracer across diverse taxa (Hall et al., 1997), including cephalopods, fish, seabirds, and marine mammals (Bustamante et al., 2006; Paula et al., 2013; Peterson et al., 2015; Le Croizier et al., 2020; Bezerra et al., 2021; Thorne et al., 2021).

This study aims to investigate the trophic interactions among eleven deep-sea fish species in the ECS using SIA combined with Hg as a complementary tracer. We hypothesized that feeding ecology drives trophic partitioning among species and analyzed trophic positions and niche overlaps to understand resource competition and coexistence mechanisms. We quantified total mercury (THg) concentrations to examine how biotic and abiotic factors (species, trophic level, ontogeny, and habitat) influence Hg accumulation. Additionally, we assessed the utility of Hg as a complementary tool in the analysis of trophic guilds (TGs), evaluating how Hg concentrations reflect feeding strategies and dynamic niche shifts within these groups. By addressing these objectives, this study seeks to enhance our understanding of the mechanisms of Hg accumulation, the trophic structure, and the potential ecological impacts on deep-sea ecosystems in the ECS.

2. Materials and methods

2.1. Sample collection and preparation

Fish samples were collected between February and April 2023 by the commercial trawler "*Zheling Fishery 74016*" in the sea area delineated by the coordinates 29°50.541′-30°36.488′N, 127°41.610′-127°57.927′E (Fig. 1). In the laboratory, all the samples were classified and identified using DNA barcoding technology, then stored at −20 °C for further analysis. The total length (TL ± 0.1 cm) and weight (±0.01 g) of each sample were measured. Fish muscles were rinsed with ultra-pure water and dried in a freeze dryer (Christ Alpha 1–4) at −55 °C for 36 h; dried tissues were then ground into a powder using a freeze mixer ball mill (Mixer mill MM440).

Eleven species were selected for this analysis: *Astronesthes chrysophekadion, Chlorophthalmus albatrossis, Coelorhynchus anatirostris, Coelorhynchus kamoharai, Congriscus megastomus, Diaphus watasei, Dicrolene tristis, Nansenia ardesiaca, Neoscopelus microchir, Polymetme elongate, Synagrops japonicus.* The biological data are presented in Table 1.

2.2. Stable isotopes analysis

SIA was carried out in the Key Laboratory of the Ministry of Education for Sustainable Exploitation of Pelagic Fishery Resources, Shanghai Ocean University.

Approximately 1.5 mg of defatted powder was weighed and encapsulated in a tin cup and subsequently was fed into a stable isotope mass spectrometer (IsoPrime 100, UK) and elemental analyser (Vario ISOTOPE cube, Germany) for stable isotope determination of carbon and nitrogen. The $\delta^{13}C$ and $\delta^{15}N$ values were calculated using the following equations:

$$\delta X = (R_{sample}/R_{standard}\text{-}1) \times 1000\ (‰) \quad (1)$$

where X is ^{13}C or ^{15}N; R_{sample} and $R_{standard}$ are the isotope ratios of the sample and the standard sample, respectively.

2.3. Total mercury (THg) analysis

The THg concentrations in all samples were determined using thermal decomposition (combustion), amalgamation, and atomic absorption spectroscopy with a calibrated DMA-80 Direct Hg Analyser (Milestone, Italy). Approximately 0.02 g of dried and homogenized powder was loaded into the DMA-80 and combusted at 650 °C in an aerobic environment. The procedure involved drying for 100 s, decomposition for 150 s, and a 10 s waiting period. Quality control procedures included analysis of laboratory method blanks, duplicate tissue samples, and certified reference materials (DORM-4) were analyzed. The precision of duplicate samples averaged ±6.56%, and the percentage recovery for the certified reference materials ranged from 95% to 108%.

2.4. Data analysis

All the results were expressed as mean ± standard deviation. Since the samples did not satisfy normality and homogeneity of variance, the Kruskal-Wallis test was used to test the variability of $\delta^{13}C$, $\delta^{15}N$ values, and THg concentrations among species. We used two-dimensional (2D) ($\delta^{13}C$ and $\delta^{15}N$) ellipse areas and three-dimensional (3D) ($\delta^{13}C$, $\delta^{15}N$, and THg) ellipsoids, encompassing 40% of the data (SEA and SEV) calculated using the SIBER package (Jackson et al., 2011) and Markov Chain Monte Carlo (MCMC), respectively.

We showed isotopic overlap as a percentage of the 2D ellipses (SEA) or 3D ellipsoids (SEV) so that we could compare the results from the two models. Following Parzanini et al. (2017), a hierarchical cluster analysis (Ward's linkage, Euclidean distance) was performed on the mean $\delta^{13}C$, $\delta^{15}N$ values, and THg concentrations for each species to identify

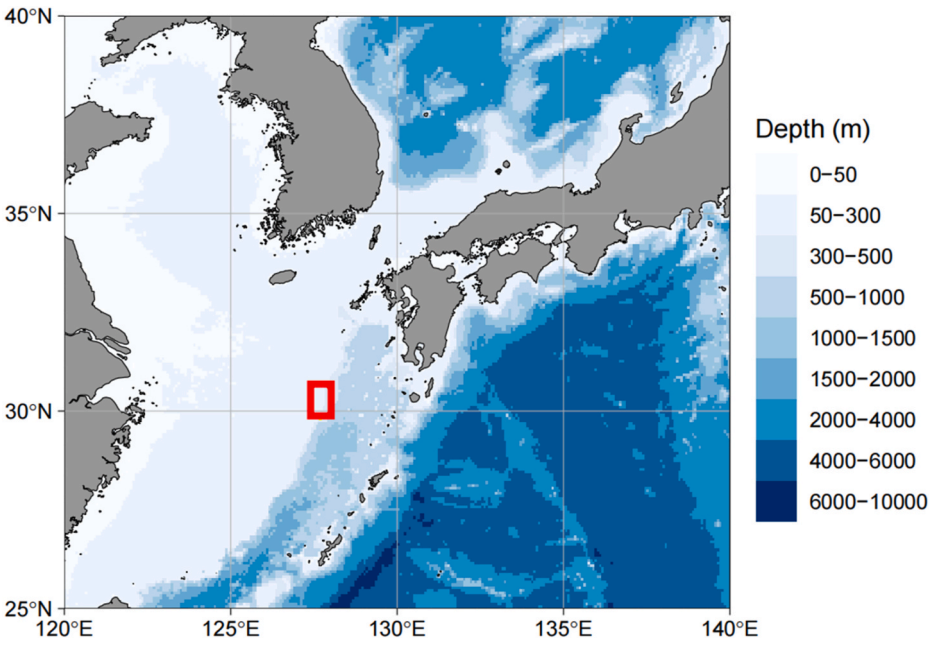

Fig. 1. Map of the study area in the ECS.

Table 1
Sampling size (n), habitat, mean total length (TL, cm), $\delta^{13}C$, $\delta^{15}N$ values (‰), trophic position (TP) and THg concentrations (mg/kg, DW) of eleven deep-sea fish species in the ECS.

Species name	n	Habitat	TL (cm)	$\delta^{13}C$ (‰)	$\delta^{15}N$ (‰)	TP	THg (mg/kg, DW)
Astronesthes chrysophekadion	21	mesopelagic	16.0 ± 1.6	−19.82 ± 1.11	10.90 ± 0.42	2.93	0.56 ± 0.24
Chlorophthalmus albatrossis	28	demersal	10.9 ± 1.4	−19.33 ± 0.24	9.73 ± 0.31	2.59	0.14 ± 0.02
Coelorhynchus anatirostris	8	demersal	19.6 ± 2.7	−17.96 ± 0.93	13.05 ± 0.86	3.56	0.78 ± 0.32
Coelorhynchus kamoharai	21	demersal	18.6 ± 3.3	−18.42 ± 0.35	11.43 ± 0.40	3.09	0.24 ± 0.15
Congriscus megastomus	16	demersal	22.2 ± 4.6	−19.80 ± 1.35	11.03 ± 0.80	2.97	0.35 ± 0.20
Diaphus watasei	31	mesopelagic	12.4 ± 2.1	−19.53 ± 0.90	11.17 ± 0.45	3.01	0.59 ± 0.22
Dicrolene tristis	7	demersal	15.7 ± 2.9	−18.69 ± 0.40	11.68 ± 0.37	3.16	0.42 ± 0.18
Nansenia ardesiaca	5	mesopelagic	12.2 ± 1.0	−20.47 ± 0.86	10.07 ± 0.71	2.69	0.15 ± 0.03
Neoscopelus microchir	9	mesopelagic	12.0 ± 3.1	−19.52 ± 0.21	10.64 ± 0.44	2.86	0.35 ± 0.14
Polymetme elongata	23	mesopelagic	15.2 ± 1.0	−17.81 ± 1.99	11.12 ± 0.36	3.00	0.19 ± 0.09
Synagrops japonicus	24	demersal	14.2 ± 1.8	−18.56 ± 0.37	10.54 ± 0.60	2.83	0.16 ± 0.06

potential functional groups or trophic niches among the species studied.

To investigate the relationship between THg and fish standard length, log_{10}-transformed THg concentrations (lgTHg) were examined against fish TL using the Pearson correlation test. The linear relationship between lgTHg and the $\delta^{15}N$ values was used to assess the biomagnification of Hg at various trophic levels according to Nfon et al. (2009). The trophic magnification factor (TMF) was calculated using the following formula:

$$TMF = 10^{b} \quad (2)$$

where b is the slope of the linear relationship between the lgTHg and $\delta^{15}N$ values, also known as the trophic magnification slope (TMS). TMF represents the increase in Hg concentration at each trophic position (TP). The TP calculation formula is as follows:

$$TP_{consumer} = (\delta^{15}N_{consumer} - \delta^{15}N_{baseline})/\Delta^{15}N + \lambda \quad (3)$$

where $TP_{consumer}$ is the trophic level of the consumer and $\delta^{15}N_{consumer}$ is its $\delta^{15}N$ value. $\delta^{15}N_{baseline}$ is the $\delta^{15}N$ value of the baseline organism, λ is the trophic level of the baseline organism and $\Delta^{15}N$ is the trophic discrimination factor (TDF). According to Zou et al. (2022), $\delta^{15}N_{baseline} = 7.73‰$, $\lambda = 2$, $\Delta^{15}N = 3.4‰$. Fish were divided into three groups based on TP: low trophic position group (LP, ≤3), medium trophic position group (MP, 3–3.5), and high trophic position group (HP, >3.5).

Generalized linear models (GLMs) were applied to assess the effects of total length (TL), habitat, $\delta^{13}C$, and $\delta^{15}N$ values on THg concentrations in the muscle tissues of deep-sea fishes. Using species distribution data from FishBase and relevant literature, the eleven species studied were classified as either mesopelagic or demersal fish (Table 1; Froese and Pauly, 2000; Staby and Salvanes, 2019). No significant relationship was detected between $\delta^{13}C$ or $\delta^{15}N$ values and TL within or across species. GLMs were constructed with the LME4 package, using THg concentration as the response variable. Residual diagnostic plots indicated the appropriateness of a Gaussian distribution and an identity link function for the models. The Akaike Information Criterion (AIC) was employed to identify the model with the best fit (lowest AIC score), and the variance inflation factor (VIF) was used to check for multicollinearity among the predictor variables.

3. Results

3.1. $\delta^{13}C$, $\delta^{15}N$ values and THg concentrations across the deep-sea fish community of the ECS

Muscle tissue $\delta^{13}C$ values differed significantly among fish species (Kruskal-Wallis, $P < 0.01$), ranging from −20.47 ± 0.86‰ in *N. ardesiaca* to −17.81 ± 1.99‰ in *P. elongata* (Table 1, Fig. S1). Interspecific variation was also observed in $\delta^{15}N$ signatures (Kruskal-Wallis, $P < 0.01$), with *C. anatirostris* showing the highest enrichment (13.05 ±

0.86‰) and *C. albatrossis* displaying the lowest values (9.73 ± 0.31‰) among all deep-sea species analyzed (Table 1, Fig. S2).

Muscle tissue THg concentrations varied significantly among the eleven studied species (Kruskal-Wallis, $P < 0.01$, Fig. S3). *C. anatirostris* displayed the highest THg levels (0.78 mg/kg DW), followed by *D. watasei* (0.59 mg/kg DW) and *A. chrysophekadion* (0.56 mg/kg DW), while *C. albatrossis* and *N. ardesiaca* showed the lowest concentrations (0.14 and 0.15 mg/kg DW, respectively) (Table 1). When converted to wet weight (WW), THg concentrations ranged from 0.01 to 0.34 mg/kg WW, remaining below the Food and Agriculture Organization (FAO) threshold (0.5 mg/kg WW).

3.2. Variation in niches of species and trophic guilds (TGs)

The isotopic niches of most species clustered closely along the $\delta^{15}N$ and $\delta^{13}C$ axes, with substantial niche overlap, except for *C. anatirostris*, which occupied a distinct position along the $\delta^{15}N$ axis (Fig. 2). Standard ellipse areas (SEAc) varied considerably among species (0.20–3.63‰^{2}), with *C. megastomus, C. anatirostris,* and *N. ardesiaca* showing the most isotopic spaces, while *C. albatrossis* and *N. microchir* exhibited the most restricted isotopic spaces (Table S1, Fig. 2). Maximum niche overlap was observed between *C. megastomus* and three species: *A. chrysophekadion, D. watasei* (both 100%), and *N. microchir* (98.33%). Conversely, *C. albatrossis* and *C. anatirostris* maintained distinct isotopic niches with minimal overlap with other species.

Hierarchical cluster analysis identified four distinct TGs among the eleven species (Fig. S4). Based on $\delta^{13}C$ values and literature evidence, TG 1 and TG 2 were characterized as demersal, while TG 3 and TG 4 were classified as mesopelagic. Initial 2D ecological niche analysis revealed substantial overlap between TG 2 and TG 3 (Fig. 3, Table S2). The incorporation of THg as a third dimension significantly modified intergroup relationships (Fig. 4, Table S3), notably reducing the TG 3-TG 2 overlap from 55.62% to 13.12%, while other intergroup overlaps showed minimal increases (<5%).

3.3. Drivers of THg variability: trophic level, size and habitat

The GLMs analysis of the entire food web showed that $\delta^{15}N$ values and habitat had the most significant effect on THg concentration, while $\delta^{13}C$ values and TL had no significant effect (Table S4 and Fig. S5). A significant relation emerged between lgTHg and $\delta^{15}N$ values across all species ($r = 0.58$, $P < 0.01$), described by $lgTHg = 0.20(\delta^{15}N) - 2.69$, where TMS = 0.20 and TMF = 1.58 (Fig. 5). Low-trophic-level species *C. albatrossis* and *N. ardesiaca* (TP = 2.59 and 2.69, respectively) had the lowest THg concentration (0.14 and 0.15 mg/kg), while the only high-trophic-level species, *C. anatirostris* (TP = 3.56), had the highest THg concentration. However, some higher trophic level species (*C. kamoharai* and *P. elongata*) displayed unexpectedly low THg concentrations. The GLMs results also showed that mesopelagic species consistently had higher THg levels than demersal species. This was true even when species from the different taxonomic groups were at the same trophic level, such as *D. watasei* vs. *C. kamoharai* and *A. chrysophekadion* vs. *C. megastomus*.

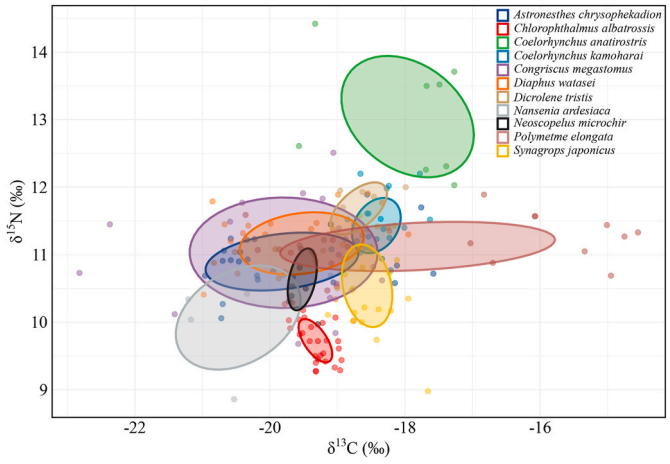

Fig. 2. Stable isotopic niches of eleven deep-sea fish species.

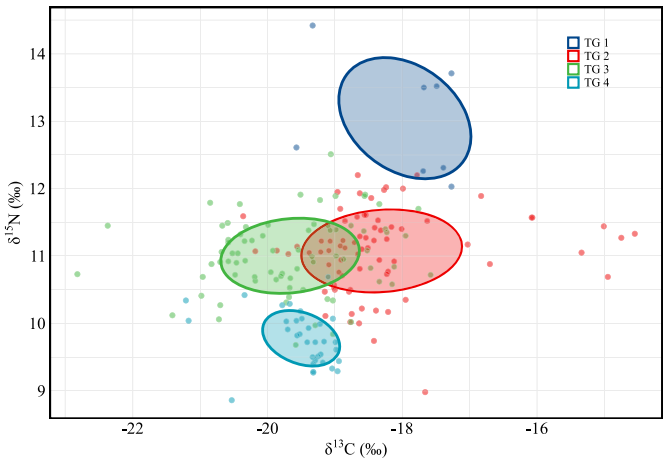

Fig. 3. 2D trophic niche plot for the four trophic guilds (TGs) based on hierarchical cluster analysis. TG 1: *C. anatirostris*; TG 2: *S. japonicus*, *C. kamoharai*, *D. tristis*, *P. elongata*; TG 3: *A. chrysophekadion*, *C. megastomus*, *D. watasei*, *N. microchir*; TG 4: *C. albatrossis*, *N. ardesiaca*.

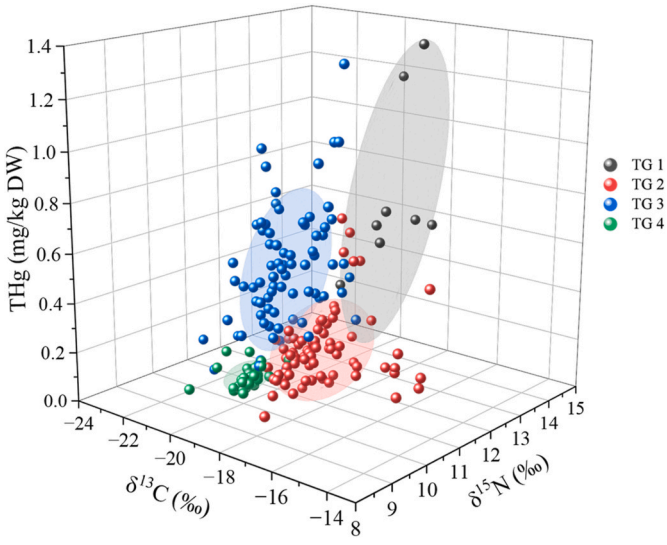

Fig. 4. 3D trophic niche plot for the four trophic guilds (TGs).

There were strong positive correlations ($P < 0.05$) between THg levels and body size in seven species (Fig. 6). Among smaller species, THg concentrations varied markedly: *C. albatrossis* (mean size 10.9 cm) contained 0.14 mg/kg DW, while *D. watasei* (mean size 12.4 cm) showed substantially higher levels at 0.59 mg/kg DW. Larger species such as *C. anatirostris* and *C. megastomus* exhibited elevated THg concentrations.

4. Discussion

4.1. Resource partitioning among the eleven deep-sea fish species

An organism's trophic niche width reflects the diversity of resources it exploits for nutrition (Bearhop et al., 2004). Tissue isotope ratios provide integrated information about both trophic position and spatial

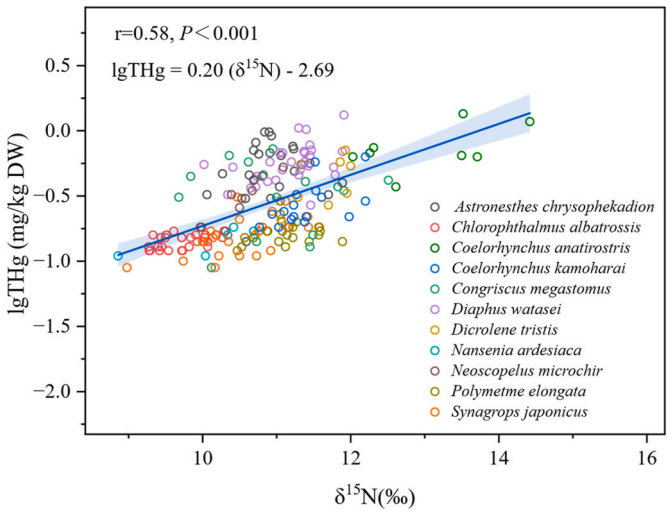

Fig. 5. Regression relationship between lgTHg and $\delta^{15}N$ values, r is the Pearson correlation coefficient with significance determined by values of $P < 0.05$. The blue area delineates the 95% confidence interval.

distribution, with $\delta^{13}C$ values serving as crucial indicators of carbon sources and changes in individual foraging habitats (Cherel and Hobson, 2007). The broad range of $\delta^{13}C$ values observed in *P. elongata* suggests ontogenetic habitat shifts to deeper water layers (Takami, 2022), similar to patterns documented in mesopelagic communities of the southern Kerguelen Plateau (Woods et al., 2020). The large isotopic niche displayed by *C. anatirostris* in a two-dimensional context indicates the exploitation of diverse food resources. This finding supports earlier stomach content analyses that identified this species as a generalist, consuming both epibenthic and endobenthic organisms (Ozawa and Zinno, 1990; Carrassón and Matallanas, 2002). In contrast, *C. albatrossis, D. tristis*, and *N. microchir* exhibited narrower isotopic niches, suggesting more specialized feeding strategies focused on a limited prey range (Ozawa and Zinno, 1990).

Trophic niche overlap refers to the degree of similarity in resource utilization and the potential for competitive interactions among species, whereas trophic niche differentiation pertains to the dietary differences and habitat segregation observed between species (Costa-Pereira et al., 2019). Stable isotope ratios found in the tissues of organisms, which reflect the cumulative effects of all trophic pathways leading to that individual, are frequently employed to characterize the trophic niche (Layman et al., 2007). *C. anatirostris* (high trophic position) and *C. albatrossis* (low trophic position) occupied distinct isotopic niches, reflecting minimal competition for food resources or habitat use between the two species. The significant niche overlap (64.55%) observed in the study area between *D. watasei* and *A. chrysophekadion* was attributed to their shared carnivorous diet, which primarily consists of small lanternfish and krill (Sutton and Hopkins, 1996), as reported by Liao et al. (2006) in the coastal waters of Taiwan.

Trophic guilds classify species based on their shared food resources and feeding strategies (Root, 1967), helping identify functional roles within ecosystems through analysis of feeding relationships and resource utilization patterns (Segura-Trujillo et al., 2016). In our 2D analysis, while TG 1 and TG 2 showed similar $\delta^{13}C$ values indicating shared habitats, their $\delta^{15}N$ differences likely reflect size-dependent prey selection (Fig. 3). Within TG 1, the larger-bodied *C. anatirostris* targets higher trophic level prey, expanding its niche and reducing interspecific competition (Woods et al., 2020). *P. elongata*'s classification in TG 2 reflects its ontogenetic migration to deeper waters, while *C. megastomus*' placement in TG 3 aligns with its predominantly mesopelagic fish diet (Ozawa and Zinno, 1990; Takami, 2022). The distinct foraging patterns between TG 2 and TG 3 manifest in their isotopic signatures. TG 2's elevated $\delta^{13}C$ values indicate deeper-water foraging, supported by substantial benthic prey consumption (Ozawa and Zinno, 1990). TG 3, which primarily feeds on small mesopelagic fishes and crustaceans, functions as a link between deep-sea and pelagic food webs, facilitating energy transfer and trophic cascades (Liao et al., 2006; Zhang and Guo, 2024). TG 4's specialization in small crustaceans contributes to zooplankton population regulation and pelagic food web stability (Ozawa and Zinno, 1990; Kudo et al., 1970).

4.2. Hg as a complementary dietary tracer

Our analysis revealed positive linear correlations between muscle tissue THg concentrations and body size in most species examined, aligning with previous findings (Storelli et al., 2006; Sackett et al., 2013; Seco et al., 2020). This pattern reflects Hg bioaccumulation through dietary exposure in mid-trophic level fish (Phillips and Buhler, 1978), as larger individuals typically consume bigger prey with higher Hg content (Chouvelon et al., 2014) and exhibit reduced Hg excretion rates (Trudel and Rasmussen, 1997). However, four species (*C. albatrossis*, *C. megastomus*, *C. kamoharai*, and *N. ardesiaca*) showed no significant length-THg correlation (Fig. 6). Sakaji et al. (2006) reported that *Chlorophthalmus* spp. enter the reproductive phase when their TL reaches between 75 and 115 mm. During ovulation, female fish may metabolize a portion of THg through the spawning process (Khadra et al., 2019). Additional factors affecting THg-size relationships include dietary stability, growth dilution effects, and Hg elimination rates (Simoneau et al., 2005; Ward et al., 2010; Dang and Wang, 2012). The limited data availability for deep-sea species constrains our ability to fully explain these patterns, highlighting critical knowledge gaps and the need for more comprehensive research into Hg bioaccumulation mechanisms.

Habitat and depth distribution are key ecological factors that influence THg concentrations in fish (Monteiro et al., 1996). It is widely accepted that THg concentrations in fish tend to increase with depth; previous studies have generally reported slightly elevated THg levels in demersal fish compared to mesopelagic fish (Romero-Romero et al., 2022). In contrast, our findings indicate that mesopelagic fish exhibit significantly higher THg concentrations than demersal fish, even among species occupying similar trophic levels (Table 1; Fig. S5). For example, substantial differences in THg concentrations were noted between *D. watasei* and *C. kamoharai*, as well as between *A. chrysophekadion* and *C. megastomus*. This unexpected pattern may be attributed to the complex spatial distribution of THg in seawater (Cossa et al., 2011). The ECS, characterized as a dynamic and variable marine system, displays highly heterogeneous THg distributions influenced by the interplay of multiple water masses, including the discharge from the Yangtze River and the Kuroshio Current (Liu et al., 2020). This heterogeneity complicates the straightforward depth-dependent increase in THg concentrations, as shallower waters are observed to have higher THg levels (Liu et al., 2020). Moreover, mesopelagic fish tend to exhibit higher feeding rates than demersal fish, likely due to their increased energy requirements to sustain a broader range of activities (Drazen and Sutton, 2017; Andresen et al., 2024). Additionally, their extensive movements may lead to exposure to areas with elevated THg concentrations, thereby enhancing THg bioaccumulation. In conclusion, the relatively high THg concentrations observed in mesopelagic fish are likely the result of a combination of environmental factors and ecological behaviors.

The lgTHg and $\delta^{15}N$ values of the eleven species examined in this study demonstrated a positive linear relationship (Fig. 5), consistent with the findings of previous research on Hg biomagnification within the ECS and other marine food webs (Matias et al., 2022; Zou et al., 2022). This positive correlation indicates that species at higher trophic levels tend to accumulate greater amounts of Hg, as summarized by McMeans et al. (2010) and Kiszka et al. (2015). Consequently, THg concentrations in organisms serve as a reliable indicator of their trophic level. This finding highlights the significance of Hg concentrations in evaluating the impact on deep-sea predators and the overall health of the ecosystem

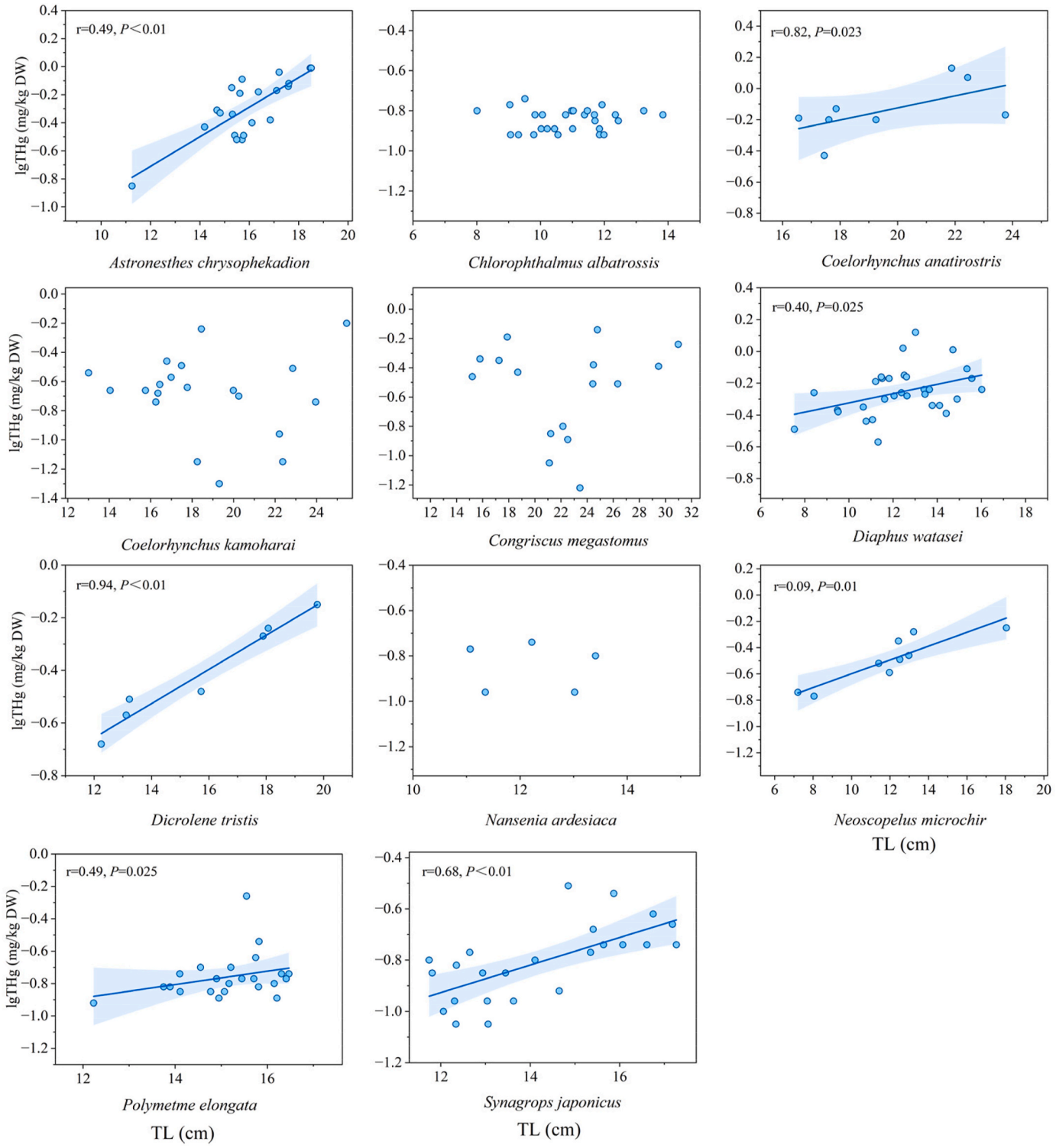

Fig. 6. Relationship between TL and lgTHg concentration in eleven species of deep-sea fish, r is the Pearson correlation coefficient with significance determined by values of $P < 0.05$. The blue area delineates the 95% confidence interval.

(Drazen and Sutton, 2017; Kozak et al., 2021).

Notably, among the species studied, *C. kamoharai* and *P. elongata*, despite their higher trophic level positions, exhibited lower THg concentrations. A similar trend has been observed in pelagic sharks, where the THg concentration in the smooth hammerhead shark (*Sphyrna zygaena*) is lower than that in the blue shark (*Prionace glauca*), which occupies a lower trophic level (Besnard et al., 2021). The $\delta^{15}N$ values not only reflect trophic levels but also indicate the $\delta^{15}N$ baseline of foraging areas (Lorrain et al., 2015). In oxygen-depleted deep waters, bacterial denitrification induces substantial $\delta^{15}N$ fractionation, enriching both residual nitrate and organic matter. Consequently, prey organisms in these depths exhibit elevated $\delta^{15}N$ signatures compared to those in the euphotic zone (Graham et al., 2010). This mechanism may explain the unexpectedly low THg concentrations in high-trophic demersal species through the combined effects of elevated $\delta^{15}N$ baselines and reduced environmental Hg availability in their habitat.

Mercury (Hg) uptake in fish occurs primarily through dietary consumption, establishing its utility as a dietary tracer in aquatic ecosystems (Seco et al., 2020; Li et al., 2022). This element serves as an effective indicator of long-term feeding patterns and bioaccumulation processes, revealing nuanced differences in species-specific foraging strategies (Dorea et al., 2006; Le Croizier et al., 2020). The incorporation of Hg data revealed a significant modification in niche overlap between TG 3 and TG 2, manifesting as a 42.5% reduction. This pattern likely reflects distinct habitat preferences and prey selection between the groups, characterized by differential Hg exposure. TG 2 predominantly targets prey with lower Hg concentrations in benthic environments, while TG 3 focuses on species with elevated Hg levels inhabiting epipelagic to mesopelagic zones. Conversely, the increased proportion between TG 1 and TG 3 suggests consumption of prey with comparable Hg levels.

Many demersal fish species exhibit opportunistic predation strategies (Dolbeth et al., 2008). For instance, *C. anatirostris* not only preys on benthic organisms but also exploits food resources from shallower layers, such as Euphausiacea, thereby enhancing the ecological niche overlap between the two groups. This phenomenon indicates that Hg incorporation reflects the ecological coupling between mesopelagic and demersal species. Consequently, the integration of Hg as a complementary measure alongside stable carbon and nitrogen isotopes in trophic niche analyses provides valuable insights into species-specific dietary strategies, habitat utilization, and food web dynamics, thereby enriching our understanding of ecological interactions (Fragoso et al., 2024).

5. Conclusion

This study highlights the importance of trophic guilds variations within the deep-sea ecosystem, reflecting distinct habitat preferences and dietary choices among species. It underscores the role of vertical niche differentiation and dietary partitioning in promoting species coexistence and ecosystem stability. Additionally, mercury (Hg) as a complementary dietary tracer revealed significant changes in trophic niche overlaps, enhancing our understanding of ecological interactions between mesopelagic and demersal groups. However, the species-specific patterns of Hg accumulation suggest the need for future research to investigate regional environmental factors, ontogenetic habitat shifts, feeding habits, and complex biogeochemical processes.

CRediT authorship contribution statement

Xinyu Chen: Writing – original draft, Methodology, Investigation, Data curation. **Zezheng Li:** Writing – review & editing, Conceptualization. **David Mboglen:** Writing – review & editing, Conceptualization. **Yunkai Li:** Writing – review & editing, Resources, Funding acquisition.

Declaration of competing interest

The authors declare that they have no known competing financial interests or personal relationships that could have appeared to influence the work reported in this paper.

Acknowledgments

This work was supported by the National Natural Science Foundation of China (#42276092) and the Program for Professor of Special Appointment (Eastern Scholar) at Shanghai Institutions of Higher Learning. The authors thank the staff at "*Zheling Fishery 74016*" for their assistance with sample collection and preparation.

Appendix A. Supplementary data

Supplementary data to this article can be found online at https://doi.org/10.1016/j.dsr.2025.104473.

Data availability

Data will be made available on request.

References

Andresen, H., Eduardo, L.N., Olivar, M.P., van Denderen, P.D., Spitz, J., Maureaud, A.A., et al., 2024. Mesopelagic fish traits: functions and trade-offs. Fish Fish. https://doi.org/10.1111/faf.12867.

Barbosa, R.V., Point, D., Médieu, A., Allain, V., Gillikin, D.P., Couturier, L.I., et al., 2022. Mercury concentrations in tuna blood and muscle mirror seawater methylmercury in the Western and Central Pacific Ocean. Mar. Pollut. Bull. 180, 113801. https://doi.org/10.1016/j.marpolbul.2022.113801.

Bearhop, S., Adams, C.E., Waldron, S., Fuller, R.A., Macleod, H., Bearhop, S., Adams, C. E., Waldron, S., Fuller, R.A., Macleod, H., 2004. Determining trophic niche width: a novel approach using stable isotope analysis. J. Anim. Ecol. 73 (5), 1007–1012. https://doi.org/10.1111/j.0021-8790.2004.00861.x.

Bernal, A., Olivar, M.P., Maynou, F., Fernández de Puelles, M.L., 2015. Diet and feeding strategies of mesopelagic fishes in the western Mediterranean. Prog. Oceanogr. 135, 1–17. https://doi.org/10.1016/j.pocean.2015.03.005.

Besnard, L., Le Croizier, G., Galván-Magaña, F., Point, D., Kraffe, E., Ketchum, J., et al., 2021. Foraging depth depicts resource partitioning and contamination level in a pelagic shark assemblage: insights from mercury stable isotopes. Environ. Pollut. 283, 117066.

Bezerra, M.F., Seminoff, J.A., Lemons, G.E., Slotton, D.G., Watanabe, K., Lai, C.T., 2021. Trophic ecology of sympatric batoid species (Chondrichthyes: batoidea) assessed by multiple biogeochemical tracers ($\delta^{13}C$, $\delta^{15}N$ and total Hg). Environ. Res. 199. https://doi.org/10.1016/j.envres.2021.111398.

Boecklen, W.J., 2011. Use of stable isotopes in foraging ecology and food web analysis. Annu. Rev. Ecol. Evol. Systemat. 42. https://doi.org/10.1146/annurev-ecolsys-102209-144726.

Brandl, S.J., Casey, J.M., Meyer, C.P., 2020. Dietary and habitat niche partitioning in congeneric cryptobenthic reef fish species. Coral Reefs 39 (2), 305–317. https://doi.org/10.1007/s00338-020-01892-z.

Bustamante, P., Lahaye, V., Durnez, C., Churlaud, C., Caurant, F., 2006. Total and organic Hg concentrations in cephalopods from the North Eastern Atlantic waters: influence of geographical origin and feeding ecology. Sci. Total Environ. 368 (2–3), 585–596. https://doi.org/10.1016/j.scitotenv.2006.01.038.

Carrassón, M., Matallanas, J., 2002. Diets of deep-sea macrourid fishes in the western Mediterranean. Mar. Ecol. Prog. Ser. 234, 215–228.

Caut, S., Angulo, E., Courchamp, F., 2009. Variation in discrimination factors ($\Delta^{15}N$ and $\Delta^{13}C$): the effect of diet isotopic values and applications for diet reconstruction. J. Appl. Ecol. 46 (2), 443–453. https://doi.org/10.1111/j.1365-2664.2009.01620.x.

Chen, Y.K., Chen, W.Y., Wang, Y.C., Lee, M.A., 2016. Winter assemblages of ichthyoplankton in the waters of the East China sea shelf and surrounding taiwan. Fish. Sci. 82 (5), 755–769. https://doi.org/10.1007/s12562-016-1012-x.

Cherel, Y., Hobson, K.A., 2007. Geographical variation in carbon stable isotope signatures of marine predators: a tool to investigate their foraging areas in the Southern Ocean. Mar. Ecol. Prog. Ser. 329, 281–287. https://doi.org/10.3354/meps329281.

Chouvelon, T., Caurant, F., Cherel, Y., Simon-Bouhet, B., Spitz, J., Bustamante, P., 2014. Species-and size-related patterns in stable isotopes and mercury concentrations in fish help refine marine ecosystem indicators and provide evidence for distinct management units for hake in the Northeast Atlantic. ICES (Int. Counc. Explor. Sea) J. Mar. Sci. 71 (5), 1073–1087. https://doi.org/10.1093/icesjms/fst199.

Cook, A.B., Sutton, T.T., Galbraith, J.K., Vecchione, M., 2013. Deep-pelagic (0–3000 m) fish assemblage structure over the mid-atlantic ridge in the area of the charlie-gibbs fracture zone. Deep Sea Res. Part II Top. Stud. Oceanogr. 98, 279–291. https://doi.org/10.1016/j.dsr2.2012.09.003.

Cossa, D., Heimbürger, L.E., Lannuzel, D., Rintoul, S.R., Butler, E.C., Bowie, A.R., et al., 2011. Mercury in the southern ocean. Geochem. Cosmochim. Acta 75 (14), 4037–4052. https://doi.org/10.1016/j.gca.2011.05.001.

Costa-Pereira, R., Araújo, M.S., Souza, F.L., Ingram, T., 2019. Competition and resource breadth shape niche variation and overlap in multiple trophic dimensions. Proc. Biol. Sci. 286. https://doi.org/10.1098/rspb.2019.0369, 1902.

Dang, F., Wang, W.X., 2012. Why mercury concentration increases with fish size? Biokinetic explanation. Environ. Pollut. 163, 192–198. https://doi.org/10.1016/j.envpol.2011.12.026.

Davison, P.C., Checkley, D.M., Koslow, J.A., Barlow, J., 2013. Carbon export mediated by mesopelagic fishes in the northeast Pacific Ocean. Prog. Oceanogr. 116, 14–30. https://doi.org/10.1016/j.pocean.2013.05.013.

Davison, P., Lara-Lopez, A., Anthony Koslow, J., 2015. Mesopelagic fish biomass in the southern California current ecosystem. Deep-Sea Res. Part II Top. Stud. Oceanogr. 112, 129–142. https://doi.org/10.1016/j.dsr2.2014.10.007.

Dolbeth, M., Martinho, F., Leitão, R., Cabral, H., Pardal, M.A., 2008. Feeding patterns of the dominant benthic and demersal fish community in a temperate estuary. J. Fish. Biol. 72 (10), 2500–2517. https://doi.org/10.1111/j.1095-8649.2008.01856.x.

Dorea, J.G., Barbosa, A.C., Silva, G.S., 2006. Fish mercury bioaccumulation as a function of feeding behavior and hydrological cycles of the Rio Negro, Amazon. Comp. Biochem. Physiol. C Toxicol. Pharmacol. 142 (3–4), 275–283. https://doi.org/10.1016/j.cbpc.2005.10.014.

Drazen, J.C., Sutton, T.T., 2017. Dining in the deep: the feeding ecology of deep-sea fishes. Ann. Rev. Mar. Sci 9 (1), 337–366. https://doi.org/10.1146/annurev-marine-010816-060543.

Fragoso, C.P., Gatts, P.V., Beneditto, A.P.M.D., Martinelli, L.A., Lacerda, L.D.D., Rezende, C.E.D., 2024. Stable isotopes and mercury as tools to depict aquatic food webs. Quim. Nova 47. https://doi.org/10.21577/0100-4042.20230125 e-20230125.

Froese, R., Pauly, D. (Eds.), 2000. Fishbase 2000: Concepts, Design and Data Sources. ICLARM, Los Baños, Philippines [updates in. http://www.fishbase.org.

Graham, B.S., Koch, P.L., Newsome, S.D., McMahon, K.W., Aurioles, D., 2010. Using isoscapes to trace the movements and foraging behavior of top predators in oceanic ecosystems. In: Isoscapes: understanding movement, pattern, and process on earth through isotope mapping, pp. 299–318. https://doi.org/10.1007/978-90-481-3354-3_14.

Gworek, B., Bemowska-Kałabun, O., Kijeńska, M., Wrzosek-Jakubowska, J., 2016. Mercury in marine and oceanic waters—a review. Water Air Soil Pollut. 227 (10). https://doi.org/10.1007/s11270-016-3060-3.

Haddock, S.H., Choy, C.A., 2024. Life in the midwater: the ecology of deep pelagic animals. Ann. Rev. Mar. Sci 16 (1), 383–416. https://doi.org/10.1146/annurev-marine-031623-095435.

Hall, B.D., Bodaly, R.A., Fudge, R.J.P., Rudd, J.W.M., Rosenberg, D.M., 1997. Food as the dominant pathway of methylmercury uptake by fish. Water Air Soil Pollut. 100, 13–24. https://doi.org/10.1023/a:1018071406537.

Irigoien, X., Klevjer, T.A., Røstad, A., Martinez, U., Boyra, G., Acuña, J.L., et al., 2014. Large mesopelagic fishes biomass and trophic efficiency in the open ocean. Nat. Commun. 5 (1), 3271. https://doi.org/10.1038/ncomms4271.

Jackson, A.L., Inger, R., Parnell, A.C., Bearhop, S., 2011. Comparing isotopic niche widths among and within communities: SIBER–Stable Isotope Bayesian Ellipses in R. J. Anim. Ecol. 80 (3), 595–602. https://doi.org/10.1111/j.1365-2656.2011.01806.x.

Kaartvedt, S., Staby, A., Aksnes, D.L., 2012. Efficient trawl avoidance by mesopelagic fishes causes large underestimation of their biomass. Mar. Ecol. Prog. Ser. 456, 1–6. https://doi.org/10.3354/meps09785.

Khadra, M., Caron, A., Planas, D., Ponton, D.E., Rosabal, M., Amyot, M., 2019. The fish or the egg: maternal transfer and subcellular partitioning of mercury and selenium in Yellow Perch (*Perca flavescens*). Sci. Total Environ. 675, 604–614. https://doi.org/10.1016/j.scitotenv.2019.04.226.

Kiszka, J.J., Aubail, A., Hussey, N.E., Heithaus, M.R., Caurant, F., Bustamante, P., 2015. Plasticity of trophic interactions among sharks from the oceanic south-western Indian Ocean revealed by stable isotope and mercury analyses. Deep Sea Res. Oceanogr. Res. Pap. 96, 49–58. https://10.1016/j.dsr.2014.11.006.

Kozak, N., Ahonen, S.A., Keva, O., Østbye, K., Taipale, S.J., Hayden, B., Kahilainen, K.K., 2021. Environmental and biological factors are joint drivers of mercury biomagnification in subarctic lake food webs along a climate and productivity gradient. Sci. Total Environ. 779. https://doi.org/10.1016/j.scitotenv.2021.146261.

Kudo, S., Toriyama, M., Okamura, O., Morita, S., 1970. Food studies of bottom fishes in continental slope of Tosawan. Bull. Nansei Reg. Fish. Res. Lab. (2), 85–103. http://fe is.fra.affrc.go.jp/publi/bull_nansei/bull_nansei0205.pdf.

Layman, C.A., Arrington, D.A., Montaña, C.G., Post, D.M., 2007. Can stable isotope ratios provide for community-wide measures of trophic structure? Ecology 88 (1), 42–48. https://doi.org/10.1890/07-1143.1.

Le Croizier, G., Lorrain, A., Sonke, J.E., Jaquemet, S., Schaal, G., Renedo, M., et al., 2020. Mercury isotopes as tracers of ecology and metabolism in two sympatric shark species. Environ. Pollut. 265, 114931. https://doi.org/10.1016/j.envpol.2020.114931.

Li, Z., Pethybridge, H.R., Gong, Y., Wu, F., Dai, X., Li, Y., 2022. Effect of body size, feeding ecology and maternal transfer on mercury accumulation of vulnerable silky shark *Carcharhinus falciformis* in the eastern tropical pacific. Environ. Pollut. 309. https://doi.org/10.1016/j.envpol.2022.119751.

Liao, Y.C., Chen, L.S., Shao, K.T., 2006. Review of the astronesthid fishes (stomiiformes: stomiidae: astronesthinae) from taiwan with a description of one new species. Zool. Stud. 45 (4), 517–528.

Liu, C., Chen, L., Liang, S., Li, Y., 2020. Distribution of total mercury and methylmercury and their controlling factors in the East China Sea. Environ. Pollut. 258, 113667. https://doi.org/10.1016/j.envpol.2019.113667.

Lorrain, A., Graham, B.S., Popp, B.N., Allain, V., Olson, R.J., Hunt, B.P., et al., 2015. Nitrogen isotopic baselines and implications for estimating foraging habitat and trophic position of yellowfin tuna in the Indian and Pacific Oceans. Deep Sea Res. Part II Top. Stud. Oceanogr. 113, 188–198. https://doi.org/10.1016/j.dsr2.2014.02.003.

Matias, R.S., Guímaro, H.R., Bustamante, P., Seco, J., Chipev, N., Fragão, J., et al., 2022. Mercury biomagnification in an antarctic food web of the antarctic peninsula. Environ. Pollut. 304, 119199. https://doi.org/10.1016/j.envpol.2022.119199.

McMeans, B.C., Svavarsson, J., Dennard, S., Fisk, A.T., 2010. Diet and resource use among Greenland sharks (*Somniosus microcephalus*) and teleosts sampled in Icelandic waters, using $\delta^{13}C$, $\delta^{15}N$, and mercury. Can. J. Fish. Aquat. Sci. 67 (9), 1428–1438. https://doi.org/10.1139/f10-072.

Mei, W., Umezawa, Y., Wan, X., Yuan, J., Sassa, C., Hidalgo, M., 2019. Feeding habits estimated from weight-related isotope variations of mesopelagic fish larvae in the Kuroshio waters of the northeastern East China Sea. ICES (Int. Counc. Explor. Sea) J. Mar. Sci. 76 (3), 639–648. https://doi.org/10.1093/icesjms/fsy016.

Monteiro, L.R., Costa, V., Furness, R.W., Santos, R.S., 1996. Mercury concentrations in prey fish indicate enhanced bioaccumulation in mesopelagic environments. Mar. Ecol. Prog. Ser. 141 (1–3), 21–25. https://doi.org/10.3354/meps141021.

Ñacari, L.A., Escribano, R., Harrod, C., Oliva, M.E., 2023. Combined use of carbon, nitrogen and sulfur stable isotopes reveal trophic structure and connections in deep-sea mesopelagic and demersal fish communities from the Southeastern Pacific Ocean. Deep Sea Res. Oceanogr. Res. Pap. 197, 104069. https://doi.org/10.1016/j.dsr.2023.104069.

Nfon, E., Cousins, I.T., Järvinen, O., Mukherjee, A.B., Verta, M., Broman, D., 2009. Trophodynamics of mercury and other trace elements in a pelagic food chain from the Baltic Sea. Sci. Total Environ. 407 (24), 6267–6274. https://doi.org/10.1016/j.scitotenv.2009.08.032.

Obrist, D., Kirk, J.L., Zhang, L., Sunderland, E.M., Jiskra, M., Selin, N.E., 2018. A review of global environmental mercury processes in response to human and natural perturbations: changes of emissions, climate, and land use. Ambio 47 (2), 116–140. https://doi.org/10.1007/s13280-017-1004-9.

Okazaki, Y., Nakata, H., 2007. Effect of the mesoscale hydrographic features on larval fish distribution across the shelf break of East China Sea. Cont. Shelf Res. 27 (10–11), 1616–1628. https://doi.org/10.1016/j.csr.2007.01.024.

Ozawa, T., Zinno, H., 1990. Studies on the bottom fishes of continental slope off Makurazaki, southern Japan, 2: stomach content analysis. Bull. Jpn. Soc. Fish. Oceanogr. 54 (3), 255–270.

Parzanini, C., Parrish, C.C., Hamel, J.F., Mercier, A., 2017. Trophic ecology of a deep-sea fish assemblage in the Northwest Atlantic. Mar. Biol. 164, 1–19. https://doi.org/10.1007/s00227-017-3236-4.

Paula, A., Di Beneditto, M., Trindade Bittar, V., De Rezende, C.E., Camargo, P.B., Kehrig, H.A., 2013. Mercury and stable isotopes ($\delta^{15}N$ and $\delta^{13}C$) as tracers during the ontogeny of *Trichiurus lepturus*. Neotrop. Ichthyol. 11 (1), 211–216. https://doi.org/10.1590/s1679-62252013000100024.

Peterson, S.H., Ackerman, J.T., Costa, D.P., 2015. Marine foraging ecology influences mercury bioaccumulation in deep-diving northern elephant seals. Proc. Biol. Sci. 282 (1810). https://doi.org/10.1098/rspb.2015.0710.

Pethybridge, H., Daley, R., Virtue, P., Butler, E.C.V., Cossa, D., Nichols, P.D., 2010. Lipid and mercury profiles of 61 mid-trophic species collected off south-eastern Australia. Mar. Freshw. Res. 61 (10), 1092–1108. https://doi.org/10.1071/MF09237.

Phillips, G.R., Buhler, D.R., 1978. The relative contributions of methylmercury from food or water to rainbow trout (Salmo gairdneri) in a controlled laboratory environment. Trans. Am. Fish. Soc. 107 (6), 853–861. https://doi.org/10.1577/1548-8659(1978)107<853:trcomf>2.0.co;2.

Prellezo, R., Corrales, X., Andonegi, E., Bald, C., Fernandes-Salvador, J.A., Iñarra, B., et al., 2024. Economic trade-offs of harvesting the ocean twilight zone: an ecosystem services approach. Ecosyst. Serv. 67. https://doi.org/10.1016/j.ecoser.2024.101633.

Romero-Romero, S., García-Ordiales, E., Roqueñí, N., Acuña, J.L., 2022. Increase in mercury and methylmercury levels with depth in a fish assemblage. Chemosphere 292, 133445. https://doi.org/10.1016/j.chemosphere.2021.133445.

Root, R.B., 1967. The niche exploitation pattern of the blue-gray gnatcatcher. Ecol. Monogr. 37 (4), 317–350.

Sackett, D.K., Cope, W.G., Rice, J.A., Aday, D., 2013. The influence of fish length on tissue mercury dynamics: implications for natural resource management and human health risk. Int. J. Environ. Res. Publ. Health 10 (2), 638–659. https://doi.org/10.3390/ijerph10020638.

Sakaji, H., Honda, H., Nashida, K., 2006. Growth and ontogenetic migration of greeneye *Chlorophthalmus albatrossis* in Tosa Bay, Pacific coast of south-western Japan. Fish. Sci. 72, 1250–1255. https://doi.org/10.1111/j.1444-2906.2006.01282.x.

Sassa, C., Tanaka, H., Ohshimo, S., 2016. Comparative reproductive biology of three dominant myctophids of the genus Diaphus on the slope region of the East China Sea. Deep-Sea Res. Part I Oceanogr. Res. Pap. 115, 145–158. https://doi.org/10.1016/j.dsr.2016.06.005.

Seco, J., Xavier, J.C., Bustamante, P., Coelho, J.P., Saunders, R.A., Ferreira, N., et al., 2020. Main drivers of mercury levels in Southern Ocean lantern fish Myctophidae. Environ. Pollut. 264. https://doi.org/10.1016/j.envpol.2020.114711.

Segura-Trujillo, C.A., Lidicker, W.Z., Álvarez-Castañeda, S.T., 2016. New perspectives on trophic guilds of arthropodivorous bats in North and Central America. J. Mammal. 97 (2), 644–654. https://doi.org/10.1093/jmammal/gyv212.

Simoneau, M., Lucotte, M., Garceau, S., Laliberté, D., 2005. Fish growth rates modulate mercury concentrations in walleye (*Sander vitreus*) from eastern Canadian lakes. Environ. Res. 98 (1), 73–82. https://doi.org/10.1016/j.envres.2004.08.002.

Staby, A., Salvanes, A.G.V., 2019. Mesopelagic fish. In: Encyclopedia of Ocean Sciences, third ed., vol. 1, pp. 283–289. https://doi.org/10.1016/B978-0-12-409548-9.11212-6 5.

Storelli, M.M., Giacominelli-Stuffler, R., Marcotrigiano, G.O., 2006. Relationship between total mercury concentration and fish size in two pelagic fish species: implications for consumer health. In: Journal of Food Protection, vol. 69. https://doi.org/10.4315/0362-028x-69.6.1402, 9.

Sutton, T.T., Hopkins, T.L., 1996. Trophic ecology of the stomiid (Pisces: stomiidae) fish assemblage of the eastern Gulf of Mexico: strategies, selectivity and impact of a top mesopelagic predator group. Mar. Biol. 127 (2), 179–192. https://doi.org/10.1007/bf00942102.

Takami, M., 2022. Ecological diversity of larval fishes: ontogeny of deep-sea demersal species. In: Fish Diversity of Japan: Evolution, Zoogeography, and Conservation. Springer Nature Singapore, Singapore, pp. 263–282. https://doi.org/10.1007/978-981-16-7427-3_15.

Tanaka, H., Sassa, C., Ohshimo, S., Aoki, I., 2013. Feeding ecology of two lanternfishes *Diaphus garmani* and *Diaphus chrysorhynchus*. J. Fish. Biol. 82 (3), 1011–1031. https://doi.org/10.1111/jfb.12051.

Thorne, L.H., Fuirst, M., Veit, R., Baumann, Z., 2021. Mercury concentrations provide an indicator of marine foraging in coastal birds. Ecol. Indic. 121. https://doi.org/10.1016/j.ecolind.2020.106922.

Trudel, M., Rasmussen, J.B., 1997. Modeling the elimination of mercury by fish. Environ. Sci. Technol. 31 (6), 1716–1722. https://doi.org/10.1021/es960609t.

Wang, Y., Zhang, H., 2023. Study on the taxonomic diversity of fish in the East China Sea hairtail national aquatic germplasm resources conservation zone. Reg. Studies Marine Sci. 68. https://doi.org/10.1016/j.rsma.2023.103241.

Ward, D.M., Nislow, K.H., Chen, C.Y., Folt, C.L., 2010. Rapid, efficient growth reduces mercury concentrations in stream-dwelling Atlantic salmon. Trans. Am. Fish. Soc. 139 (1), 1–10. https://doi.org/10.1577/T09-032.1.

Woods, B., Walters, A., Hindell, M., Trebilco, R., 2020. Isotopic insights into mesopelagic niche space and energy pathways on the southern Kerguelen Plateau. Deep-Sea Res. Part II Top. Stud. Oceanogr. 174. https://doi.org/10.1016/j.dsr2.2019.104657.

Xu, Y., Ma, L., Sun, Y., Li, X., Wang, H., Zhang, H., 2019. Spatial variation of demersal fish diversity and distribution in the East China Sea: impact of the bottom branches of the Kuroshio Current. J. Sea Res. 144, 22–32. https://doi.org/10.1016/j.seares.2018.11.003.

Zhang, C., Guo, H., 2024. Age, growth and feeding habit of watases lanternfish *Diaphus watasei* (pisces: myctophidae) in the East China sea. Fish. Sci. 1–10. https://doi.org/10.1007/s12562-024-01796-9.

Zou, C., Yin, D., Wang, R., 2022. Mercury and selenium bioaccumulation in wild commercial fish in the coastal East China Sea: selenium benefits versus mercury risks. Mar. Pollut. Bull. 180. https://doi.org/10.1016/j.marpolbul.2022.113754.